HHS Public Access

Author manuscript

Epilepsia. Author manuscript; available in PMC 2022 June 01.

Published in final edited form as:

Epilepsia. 2021 June ; 62(6): e82–e87. doi:10.1111/epi.16913.

Homozygous *SCN1B* variants causing early infantile epileptic encephalopathy 52 affect voltage-gated sodium channel function

Marcello Scala[1,2], **Stephanie Efthymiou**[2], **Tipu Sultan**[3], **Jolien De Waele**[4], **Marta Panciroli**[2], **Vincenzo Salpietro**[1,2], **Reza Maroofian**[2], **Pasquale Striano**[1,5], **Filip Van Petegem**[6], **Henry Houlden**[2], **Frank Bosmans**[4]

[1]Department of Neurosciences, Rehabilitation, Ophthalmology, Genetics, and Maternal and Child Health, University of Genoa, Genoa, Italy

[2]Department of Neuromuscular Disorders, Institute of Neurology, University College London, London, UK

[3]Department of Pediatric Neurology, Children's Hospital and Institute of Child Health Lahore, Lahore, Pakistan

[4]Faculty of Medicine and Health Sciences, Department of Basic and Applied Medical Sciences, Ghent University, Ghent, Belgium

[5]Pediatric Neurology and Muscular Diseases Unit, G. Gaslini Institute, Genoa, Italy

[6]Department of Biochemistry and Molecular Biology, Life Sciences Institute, University of British Columbia, Vancouver, British Columbia, Canada

Abstract

We identified nine patients from four unrelated families harboring three biallelic variants in *SCN1B* (NM_001037.5: c.136C>T; p.[Arg46Cys], c.178C>T; p.[Arg60Cys], and c.472G>A; p.[Val158Met]). All subjects presented with early infantile epileptic encephalopathy 52 (EIEE52), a rare, severe developmental and epileptic encephalopathy featuring infantile onset refractory seizures followed by developmental stagnation or regression. Because *SCN1B* influences neuronal excitability through modulation of voltage-gated sodium (Na_V) channel function, we examined the effects of human $SCN1B^{R46C}$ ($\beta 1^{R46C}$), $SCN1B^{R60C}$ ($\beta 1^{R60C}$), and $SCN1B^{V158M}$ ($\beta 1^{V158M}$) on the three predominant brain Na_V channel subtypes $Na_V1.1$ (*SCN1A*), $Na_V1.2$ (*SCN2A*), and $Na_V1.6$ (*SCN8A*). We observed a shift toward more depolarizing potentials of conductance–

Correspondence Henry Houlden, UCL Queen Square Institute of Neurology, Queen Square, London WC1N 3BG, UK. h.houlden@ucl.ac.uk; Frank Bosmans, Department of Basic and Applied Medical Sciences, Ghent University, Corneel Heymanslaan 10, Ghent 9000, Belgium. frank.bosmans@ugent.be.

AUTHOR CONTRIBUTIONS

Marcello Scala and Frank Bosmans designed and performed the research, analyzed the data, and wrote and revised the paper. Marcello Scala, Marta Panciroli, Stephanie Efthymiou, and Reza Maroofian collected and analyzed genetic data. Marcello Scala, Stephanie Efthymiou, and Pasquale Striano reviewed and characterized the electroclinical phenotype of the studied families. Jolien De Waele made channel constructs and performed two-electrode voltage-clamp recording, analysis of channel activity, protein biochemistry experiments, and statistical analysis. Filip Van Petegem generated three-dimensional modeling data. Tipu Sultan, Vincenzo Salpietro, Pasquale Striano, Henry Houlden, and Frank Bosmans supervised the research and revised the paper.

CONFLICT OF INTEREST

None of the authors has any conflict of interest to disclose.

SUPPORTING INFORMATION

Additional supporting information may be found online in the Supporting Information section.

voltage relationships ($Na_V1.2/\beta1^{R46C}$, $Na_V1.2/\beta1^{R60C}$, $Na_V1.6/\beta1^{R46C}$, $Na_V1.6/\beta1^{R60C}$, and $Na_V1.6/\beta1^{V158M}$) and channel availability ($Na_V1.1/\beta1^{R46C}$, $Na_V1.1/\beta1^{V158M}$, $Na_V1.2/\beta1^{R46C}$, $Na_V1.2/\beta1^{R60C}$, and $Na_V1.6/\beta1^{V158M}$), and detected a slower recovery from fast inactivation for $Na_V1.1/\beta1^{V158M}$. Combined with modeling data indicating perturbation-induced structural changes in *β1*, these results suggest that the *SCN1B* variants reported here can disrupt normal Na_V channel function in the brain, which may contribute to EIEE52.

Keywords

developmental and epileptic encephalopathy; early infantile epileptic encephalopathy 52; EIEE52; *SCN1B* ; voltage-gated sodium channel

1 | INTRODUCTION

In humans, inherited heterozygous *SCN1B* variants have been associated with mild-to-moderate epileptic disorders within the genetic epilepsy with febrile seizures plus (GEFS+) spectrum. In contrast, biallelic variants cause early infantile epileptic encephalopathy 52 (EIEE52; Online Mendelian Inheritance in Man database #617350), characterized by infantile onset refractory seizures followed by cognitive decline and neurological features such as hypotonia, spasticity, and ataxia.1-5 Only a few individuals with EIEE52 have been reported so far, and a disease-causing mechanism remains unclear. *SCN1B* encodes for *β1*, an immunoglobulinlike molecule that modulates the function of voltage-gated sodium (Na_V) channels, a family of nine membrane proteins responsible for initiating and propagating action potentials.5,6 As such, mutations in *β1*, as well as Na_V channels, have been linked to epilepsy syndromes.5,7 We report nine EIEE52 patients from four unrelated Pakistani families that harbor three *SCN1B* variants identified by whole exome sequencing. We examined the effects of these mutations on the biophysical properties of the ubiquitous brain Na_V channel subtypes $Na_V1.1$ (*SCN1A*), $Na_V1.2$ (*SCN2A*), and $Na_V1.6$ (*SCN8A*). Our results reveal perturbation-induced alterations in multiple channel gating parameters that can be correlated to structural changes in *β1*. Altogether, these data lay the foundation for further studies into a putative relationship between aberrant *SCN1B* function and EIEE52.

2 | MATERIALS AND METHODS

2.1 | Patient ascertainment

The study was approved by the University College London Institutional Review Board. Written informed consent was obtained from parents. Nine subjects from four unrelated consanguineous families presenting with similar epileptic encephalopathies were investigated using exome sequencing.

2.2 | Exome sequencing and analysis

Genomic DNA was extracted from peripheral blood leukocytes using the QIAamp DNA Blood Midi Kit as previously described.8 Priority was given to rare biallelic functional variants with an allele frequency less than .001% in public databases (gnomAD, GME Variome, Iranome, and our in-house database of 15 500 exomes), according to a plausible

recessive mode of inheritance. Sanger sequencing was performed for variant validation and parental segregation.

2.3 | Channel electrophysiology

Human (h) $hNa_V1.1$ (NM_001165963.1, *SCN1A*), $hNa_V1.2$ (NM_021007.2, *SCN2A*), $hNa_V1.6$ (NM_014191.3, *SCN8A*), and h$\beta 1$ (NM_001037.5) were expressed and tested as previously described.9 Significance of all data was analyzed using two-way analysis of variance with post hoc Bonferroni correction. Individual time point values were analyzed using two-way Student *t*-test. Obtained values reflect the mean, and error bars reflect SEM. Additional information on data acquisition can be found in Appendix S1.

3 | RESULTS

3.1 | Epileptic phenotype

We identified nine patients from four unrelated consanguineous families of Pakistani ancestry (Families A–D; Figure 1A, Table S1). Family A consists of two affected siblings, a 9-year-old male (Patient 1) and a 5-year-old female (Patient 2), born to healthy parents. After normal psychomotor development in the first 6 months after birth, both patients started to suffer from recurrent myoclonic and generalized tonic–clonic seizures (GTCS). Subsequently, they showed developmental stagnation and regression by the age of 3 years, lacking speech and social interaction. Physical examination revealed generalized spasticity and hyperreflexia. Seizures were refractory to antiepileptic drugs (AEDs), including carbamazepine and clonazepam. Electroencephalographic (EEG) recordings at age 3 years revealed multifocal epileptic abnormalities within diffusely slowed and dysregulated cerebral activity. Family B consists of three affected children: a 6-year-old female (Patient 3) and two males (Patients 4 and 5) aged 5 and 1.5 years with healthy parents. In addition to developmental delay after birth, the patients started to suffer from GTCS by the age of 5 months followed by developmental stagnation. They were nonverbal, microcephaly was present in two subjects (Patients 4 and 5, range = −2.17 to −3.92 SD), and they all had hyperreflexia. Brain magnetic resonance imaging (MRI) was unremarkable. Their EEG recordings showed low-voltage cerebral activity intermixed with suppression–burst patterns from age 6 months up to 4 years (Figure S1). In all individuals, seizures were extremely refractory despite the use of several AEDs used alone or in combination. Family C consists of two affected females (Patients 6 and 7), deceased at the ages of 2 years and 7 months, born to healthy parents. After a regular neonatal course, both children were diagnosed with psychomotor delay and started to suffer from seizures. Subsequently, they showed developmental stagnation and regression. Seizures were resistant to AEDs. Both patients prematurely died due to unspecified epilepsy-related complications. Family D (Figure 1A, Table S1) consists of two affected females, aged 3 years (Patient 8) and 9 months (Patient 9), with healthy parents. A healthy brother and sister were deceased at 11 months due to unknown causes. Both patients suffered from focal motor seizures and were diagnosed with global developmental delay. Seizures were refractory to multidrug treatment. Neurological examination revealed hyperreflexia in both cases, and a brain MRI showed hydrocephalus in Patient IV:3. Their EEG at age 12 months revealed globally slowed cerebral activity and

theta polymorphic activity intermixed with slow waves over the posterior regions (Figure S2).

3.2 | Exome sequencing results

After exome sequencing, three different missense variants in homozygosity in *SCN1B* were deemed the most plausible causative factor in the studied families: NM_001037.5: c.136C>T; p.(Arg46Cys) in Family A, NM_001037.5: c.472G>A; p.(Val158Met) in Families B and C, and c.178C>T; p.(Arg60Cys) in Family D. These variants are rare in public databases and affect conserved residues within or close to the immunoglobulin domain (Figure 1B, Genomic Evolutionary Rate Profiling score = 3.82–4.09). They are predicted to be pathogenic by in silico tools (Table S2). Familial segregation analysis confirmed biparental inheritance.

3.3 | Effects of *SCN1B* variants on $hNa_V1.1$, $hNa_V1.2$, and $hNa_V1.6$ channels

We examined the effects of all three *β1*-subunit mutations on $Na_V1.1$, $Na_V1.2$, and $Na_V1.6$, which are predominantly expressed in the central nervous system.6,10 We recorded and compared gating parameters such as the conductance–voltage (G-V) relationship, channel availability, fast inactivation time constant (τ), and recovery from fast inactivation (RFI). We found all *β1*-subunits trafficked to the membrane (Figure S3) and that the G-V relationships (Figure 2, Figure S4, Table S3) of $Na_V1.2/\beta1^{R46C}$, $Na_V1.2/\beta1^{R60C}$, $Na_V1.6/\beta1^{R46C}$, $Na_V1.6/\beta1^{R60C}$, and $Na_V1.6/\beta1^{V158M}$ are shifted to more depolarized potentials (±9 mV, $p < .01$; ±5 mV, $p < .05$; ±5 mV, $p < .01$; ±10 mV, $p < .001$; and ±5.5 mV, $p < .001$, respectively) compared to $\beta1^{WT}$. Also, channel availability of $Na_V1.1/\beta1^{R46C}$, $Na_V1.1/\beta1^{V158M}$, $Na_V1.2/\beta1^{R46C}$, $Na_V1.2/\beta1^{R60C}$, and $Na_V1.6/\beta1^{V158M}$ is shifted to more positive potentials (±3 mV, $p < .05$; ±3 mV, $p < .05$; ±6 mV, $p < .01$; ±8 mV, $p < .01$; and ±3 mV, $p < .05$, respectively) compared to $\beta1^{WT}$. RFI measurements (Figure 2) of $Na_V1.1/\beta1^{V158M}$ show a slower channel recovery (±4 ms, $p < .01$). The RFI results of $Na_V1.2/\beta1^{V158M}$ show few individual time points that have a significantly faster recovery compared to $\beta1^{WT}$, but the half-life time of the fit was not significantly different from $\beta1^{WT}$. For τ (Figure 2), we observed several individual significant data points, although the half-life time of the fit of both *SCN1B* variants was not significantly different from $\beta1^{WT}$. Surprisingly, τ values for $Na_V1.2/\beta1^{R60C}$ showed a consistent U-shaped voltage dependence, with the fastest inactivation observed around −20 mV.

We then mapped *SCN1B* R46C/V158M mutations on available Na_V channel cryogenic electron microscopic structures including $Na_V1.2$[11] and $Na_V1.7$[12], of which the latter is in complex with *β1* (Figure 1B). A superposition of $Na_V1.2$ and $Na_V1.7$ shows that channel residues involved in binding *β1* are conserved, allowing us to make a hybrid model of $Na_V1.2$ with *β1* bound. This shows that Arg46 is a critical residue, making ionic interactions with an Asp in $Na_V1.2$ (D1693, corresponding to D1677 in $Na_V1.7$). The R46C sequence variant is thus predicted to significantly weaken these interactions. Val158 is located at the top of the transmembrane helix of *β1*. As this residue does not directly contact the Na_V channel (Figure 1B), the impact of the V158M sequence variant may involve altered membrane interactions.

4 | DISCUSSION

Although the role of heterozygous *SCN1B* variants in temporal epilepsy and GEFS+ is well established, the scenario in subjects harboring biallelic variants is more complex. In rare cases, Dravet syndrome has been reported in these individuals2,3,8; however, a distinct association between homozygous *SCN1B* variants and a severe epileptic encephalopathy is now emerging. Nine individuals from seven unrelated families have been reported (Table S1), including a subject whose Dravet syndrome was reclassified to early infantile epileptic encephalopathy given the severe epileptic phenotype, cognitive decline, and premature death.2-4,8 Recurrent clinical features are early infantile onset seizures followed by psychomotor stagnation or regression, microcephaly, axial hypotonia, appendicular spasticity, and nonspecific brain atrophy. Seizure semiology and EEG features in EIEE52 are variable (Table S1). The response to AEDs is generally poor, and epilepsy remains refractory in most cases.2-4,8 Similar to Aeby et al.,1 developmental delay was present before seizure onset in Families B, C, and D. Together with the identification of neuronal pathfinding deficits in *SCN1b*-null mice before epilepsy onset,13 these observations are consistent with preexisting brain dysfunction and support the idea that *SCN1B*-related encephalopathy should be more comprehensively considered as a developmental epileptic encephalopathy. Hence, effective seizure control might exert a less dramatic impact on the overall cognitive performances in comparison to other, similar conditions.

Electrophysiological analysis of $SCN1B^{R46C}$, $SCN1B^{R60C}$, and $SCN1B^{V158M}$ showed a complex effect on neuronal Na_V channel gating (Figure 2). Although there is still much to unravel about the underlying causal relationship, most *SCN1B* variants leading to changes in Na_V channel gating or kinetics are predicted to increase neuron excitability (see Aeby et al.,1 Patino et al.,3 Chen et al.,14 and supplementary references 4-10, Appendix S1). In concert, previous studies on Na_V channel variants linked to epilepsy syndromes assumed hyperexcitability as the underlying mechanism.15,16 However, recent work uncovered epilepsy-linked Na_V channel mutants causing a depolarizing shift in voltage dependence of channel activation and inactivation, with or without delayed recovery from inactivation, thereby illustrating the complexities associated with defining causal connections.15,17,18 Assuming that the effects of $SCN1B^{R46C}$, $SCN1B^{R60C}$, *and* $SCN1B^{V158M}$ remain the same in vivo, it is not unreasonable to postulate that action potentials are also modulated by these *SCN1B* perturbations and contribute to EIEE52.5,7,14,17 Further studies at a neuronal network level in the brain are needed to get a grasp on the link between loss or gain of function and pathologies.

In conclusion, we show an abnormal gating of human Na_V channels as a possible result of *β1* perturbations, supporting the role of *SCN1B* variants in epileptogenesis. Furthermore, we refined the molecular and phenotypic spectrum of the severe encephalopathy caused by biallelic *SCN1B* variants. The results of this study also suggest that the response to AEDs in *SCN1B*-related disorders is challenging to predict due to the complex effects of β-subunits on Na_V channel function. Additional cases will help to establish the best therapeutic approaches in *SCN1B* mutant patients.

Supplementary Material

Refer to Web version on PubMed Central for supplementary material.

ACKNOWLEDGMENTS

The authors thank the patients' families for their support and consent to the publication of this study. This research was conducted as part of the Queen Square Genomics group at University College London, supported by the National Institute for Health Research University College London Hospitals Biomedical Research Centre. We also thank Lisa Huckriede for help with electrophysiology experiments.

Funding information

This study was funded by the Medical Research Council (MR/S01165X/1, MR/S005021/1, G0601943), National Institute for Health Research University College London Hospitals Biomedical Research Centre, Rosetree Trust, Ataxia UK, MSA Trust, Brain Research UK, Sparks GOSH Charity, Muscular Dystrophy UK, Muscular Dystrophy Association (USA), Canadian Institutes of Health Research (PJT-148632; FVP), and a National Institutes of Health (USA) grant (R01NS091352) to F.B.

REFERENCES

1. Aeby A, Sculier C, Bouza AA, Askar B, Lederer D, Schoonjans AS, et al. SCN1B-linked early infantile developmental and epileptic encephalopathy. Ann Clin Transl Neur. 2019;6(12):2354–67.
2. Ogiwara I, Nakayama T, Yamagata T, Ohtani H, Mazaki E, Tsuchiya S, et al. A homozygous mutation of voltage-gated sodium channel beta(I) gene SCN1B in a patient with Dravet syndrome. Epilepsia. 2012;53:e200–3. [PubMed: 23148524]
3. Patino GA, Claes LRF, Lopez-Santiago LF, Slat EA, Dondeti RSR, Chen CL, et al. A functional null mutation of SCN1B in a patient with Dravet syndrome. J Neurosci. 2009;26(29):10764–78.
4. Ramadan W, Patel N, Anazi S, Kentab AY, Bashiri FA, Hamad MH, et al. Confirming the recessive inheritance of SCN1B mutations in developmental epileptic encephalopathy. Clin Genet. 2017;92:327–31. [PubMed: 28218389]
5. O'Malley HA, Isom LL. Sodium channel beta subunits: emerging targets in channelopathies. Annu Rev Physiol. 2015;77:481–504. [PubMed: 25668026]
6. Ahern CA, Payandeh J, Bosmans F, Chanda B. The hitchhiker's guide to the voltage-gated sodium channel galaxy. J Gen Physiol. 2016;147:1–24. [PubMed: 26712848]
7. Kaplan DI, Isom LL, Petrou S. Role of sodium channels in epilepsy. Cold Spring Harbor Perspect Med. 2016;6(6):a022814.
8. Yang YP, Muzny DM, Reid JG, Bainbridge MN, Willis A, Ward PA, et al. Clinical whole-exome sequencing for the diagnosis of Mendelian disorders. N Engl J Med. 2013;17(369):1502–11.
9. Gilchrist J, Dutton S, Diaz-Bustamante M, McPherson A, Olivares N, Kalia J, et al. Nav1.1 modulation by a novel triazole compound attenuates epileptic seizures in rodents. ACS Chem Biol. 2014; 16(9):1204–12.
10. Whitaker WR, Clare JJ, Powell AJ, Chen YH, Faull RL, Emson PC. Distribution of voltage-gated sodium channel alpha-subunit and beta-subunit mRNAs in human hippocampal formation, cor-tex, and cerebellum. J Comp Neurol. 2000;19(422):123–39.
11. Pan XJ, Li ZQ, Huang XS, Huang GXY, Gao S, Shen HZ, et al. Molecular basis for pore blockade of human Na+ channel Nav1.2 by the mu-conotoxin KIIIA. Science. 2019;22(363):1309.
12. Shen H, Liu D, Wu K, Lei J, Yan N. Structures of human Nav1.7 channel in complex with auxiliary subunits and animal toxins. Science. 2019;22(363):1303–8.
13. Brackenbury WJ, Yuan YK, O'Malley HA, Parent JM, Isom LL. Abnormal neuronal patterning occurs during early postnatal brain development of Scn1b-null mice and precedes hyperexcitability. Proc Natl Acad Sci U S A. 2013;110(3):1089–94. [PubMed: 23277545]
14. Chen C, Dickendesher TL, Oyama F, Miyazaki H, Nukina N, Isom LL. Floxed allele for conditional inactivation of the voltage-gated sodium channel beta 1 subunit Scn1b. Genesis. 2007;45:547–53. [PubMed: 17868089]

15. Begemann A, Acuna MA, Zweier M, Vincent M, Steindl K, Bachmann-Gagescu R, et al. Further corroboration of distinct functional features in SCN2A variants causing intellectual disability or epileptic phenotypes. Mol Med. 2019;25(1):6. [PubMed: 30813884]

16. Lauxmann S, Verbeek NE, Liu YY, Zaichuk M, Muller S, Lemke JR, et al. Relationship of electrophysiological dysfunction and clinical severity in SCN2A-related epilepsies. Hum Mutat. 2018;39:1942–56. [PubMed: 30144217]

17. Barela AJ, Waddy SP, Lickfett JG, Hunter J, Anido A, Helmers SL, et al. An epilepsy mutation in the sodium channel SCN1A that decreases channel excitability. J Neurosci. 2006;8(26):2714–23.

18. Zaman T, Abou Tayoun A, Goldberg EM. A single-center SCN8A-related epilepsy cohort: clinical, genetic, and physiologic characterization. Ann Clin Transl Neur. 2019;6:1445–55.

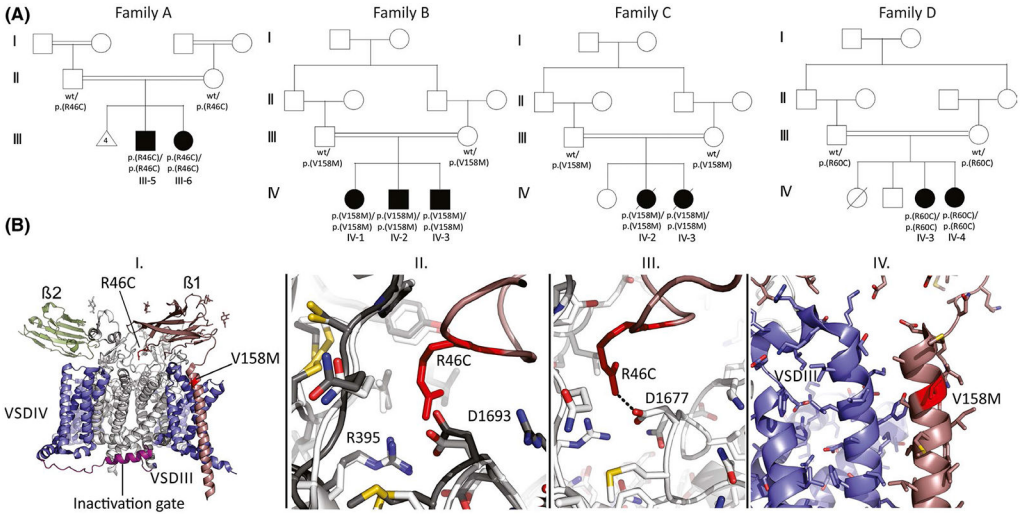

FIGURE 1.

Pedigrees of the studied families and *SCN1B* variant modeling. (A) multigeneration pedigrees of families A–D showing parental consanguinity and history of recurrent Family A miscarriages. (B) I. Three-dimensional model of $Na_V1.7$ channel encompassing *β1* (brown) and *β2* (green) subunits. The location of the R46C and V158M mutations in *SCN1B* (NM_001037.5) is indicated. II. Superposition of $Na_V1.2$ (dark) and $Na_V1.7$ (light) at the contact area for Arg46 in *β1*, showing that the interface is conserved. Arg46 makes multiple contacts with the channel. III. Dotted line represents an ionic interaction between Arg46 in *β1* and Asp1677 in $Na_V1.7$ (corresponding to Asp1693 in $Na_V1.2$). IV. Structural details around the *β1* residue V158 are shown

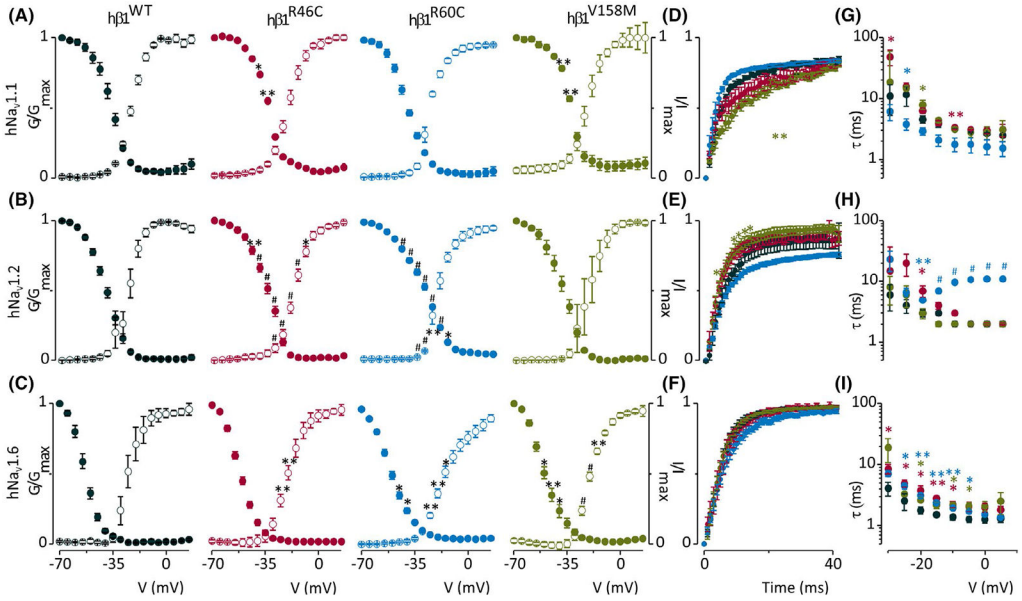

FIGURE 2.

Functional characterization of *SCN1B* missense variants. (A–C) Normalized conductance-voltage (G-V; open circles) and channel availability relationship (I-V; filled circles) of $\beta 1^{WT}$ (black), $\beta 1^{R46C}$ (red), $\beta 1^{R60C}$ (blue), or $\beta 1^{V158M}$ (green) coexpressed with human (h) $Na_V1.1$, $Na_V1.2$ or $Na_V1.6$. G-V and I-V $V_{1/2}$ values are reported in Table S3. (D–F) Normalized recovery from fast inactivation using the same color scheme measured over a 40-ms timeframe using a double-pulse protocol to the maximum current of the I-V in A–C. Half-life recovery time points (ms) are presented in Table S3. Error bars are SEM with n = 5–11; $^{*}p < .05$, $^{**}p < .01$, $^{\#}p < .001$. (G–I) Rate (τ) of channel fast inactivation. Half-life time points (ms) are presented in Table S3. Error bars reflect SEM with n = 5–6; $^{*}p < .05$, $^{**}p < .01$, $^{\#}p < .001$